Dynamic Thermal Models for Human Body Dissipation

KAROLJ SKALA
TOMISLAV LIPIĆ
IVAN SOVIĆ
IVAN GRUBIŠIĆ

Centre for Informatics and Computing,
Ruđer Bošković Institute, Zagreb, Croatia

Correspondence:
prof. dr. sc. Karolj Skala
Center for Informatics and Computing
Ruđer Bošković Institute
Zagreb, Croatia
E-mail: skala@irb.hr
http://www.irb.hr/cir

Key words: IR thermography, 3D thermal imaging; 3D thermal model; skeleton detection; mesh optimisation; human body dissipation

Abstract

The IR emissivity of human skin is extremly high and measurements of infrared radiation emitted by the skin can be converted directly into accurate temperature value. This process is known as Body IR Thermography. Skin temperature increase associated with increased vascular flow and increased metabolism. In this paper a novel multi-resolution real-time 3D thermal imaging system as potential solution for a human body 3D thermal models standardisation is presented. The system consists of a high-resolution offline 3D scanner and a real-time low-resolution 3D scanner, both of them paired together with a thermal imaging camera. The emphasis of this paper is the presentation of the novel concept of the standardisation of human body 3D thermal models, captured by the multi-resolution real-time 3D thermal imaging system. The standardisation procedure utilises skeleton detection, skeleton transformation, mesh optimisation, and texture mapping. The presented concept enables novel and practical methods for human body 3D thermal models comparison and analysis.

1. INTRODUCTION

Infrared imaging (IR), or simply thermography, is an extremely sensitive diagnostic test that measures and records surface temperature and natural heat distribution in the body. The applications of thermography in medicine for the diagnosis of various disease processes have expanded over the past decade coincident with technological advances in thermal imaging.

The medical use of IR is not new. However, with the recently improved sensitivity (around 0.02 degree Celsius) of the new generation of infrared sensors, IR is beginning to be a safe, efficient and reliable method for the study of some human diseases[1].

Infrared thermography also known as thermal imaging can provide accurate, nondestructive information about the thermal envelope performance (thermal texture) of any objects or organism. This includes validation of structural details, verification of energy performance (conduction and air leakage), location of moisture intrusion, and the identification of energy dissipation.

Our aim is a non-invasive imaging technology to allow monitoring of energy dissipation processes at organism. This technology is based on integration of visible 3D imaging and thermal imaging principles. Thermography has been used for decades by biologist and clinicians to assist with diagnosis of biomechanical and medical physiology problems. New 5D Dynamic thermography technology represent the enhanced imaging which provide quantifiable multidimensional and multispectral data sets.

The dissipation of thermal radiation can be observed by the means of *thermal infrared* (*IR*) *cameras* (in continuation: *thermal camera*). Thermal cameras generate images representing the distribution of thermal infrared radiation on the surface of objects through a process called *thermal imaging* (or short, *thermography*). Thermal imaging spans a wide range of applications from industry *(1, 2)* and medicine. Medicinal applications are especially interesting, as the physiological state of the human body greatly reflects on the temperature distribution on its surface *(3)* and can be seen as a clear indicator of bodily dysfunction *(4)*.

Analysing the surface temperature distribution from a single thermal image (thermogram) is referred to as static thermal imaging commonly used to determine the current thermal state of an object or an organism *(5)*. Some thermal processes either need to be monitored over certain time periods, or exhibit change rates which cannot be approximated as static. For this purpose, dynamic thermal imaging (DTI) is applied *(4)*. DTI can be performed in a passive or in an active manner. Passive DTI includes monitoring of only the thermal energy irradiated by the observed body *(6,7)* while in active DTI external modification of the body's temperature is applied *(8)*, such as heating or cooling the observed body.

DTI raises the question of accurate comparison and analysis of a series of thermal images, as well as repeatability of measurements and comparison of thermal images from a number of different subjects. Several thermal standardisation protocols for capturing a series of thermograms from the whole body for ROI analysis have been proposed *(9)*. However, such ROI analysis from planar thermal images can produce incorrect results due to loss of information if 3D shape of the body is not considered.

A solution for the thermogram standardisation problem can be provided in the form of a 3D thermal imaging system, that combines 3D scanning techniques *(10)* with thermal imaging, producing 3D models with thermograms as surface textures *(11, 12, 13)*. The knowledge of depth data can significantly influence the complexity and performance of tasks such as body part classification and ROI detection *(14)*.

In this paper, a concept of the standardisation of human body 3D thermal models is presented using a multi-resolution real-time 3D thermal imaging system. First, a detailed description of the multi-resolution real-time 3D thermal imaging system is given. Afterwards, the concept of standardisation procedure of human body 3D thermal models is presented.

2. MULTI-RESOLUTION REAL-TIME 3D THERMAL IMAGING SYSTEM

A common approach to 3D thermal imaging combines a 3D scanning device with a thermal camera as shown in Figure 1(a), in order to obtain 3D models with temperature distribution as surface textures. Multi-resolution real-
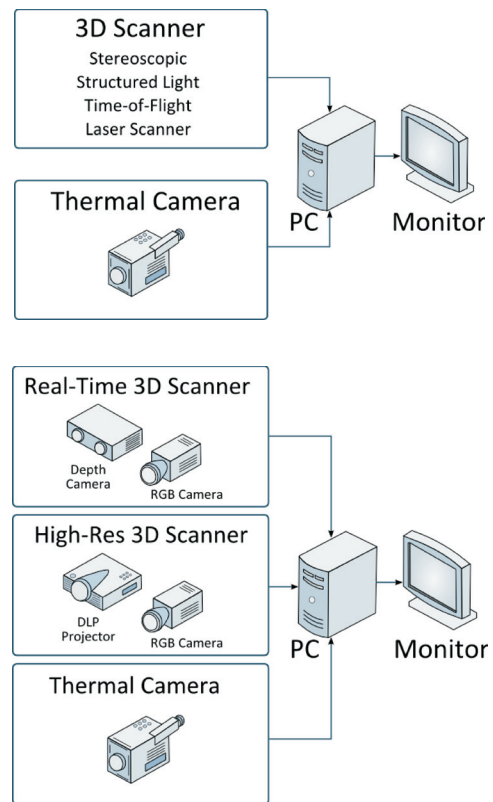

Figure 1. *The configuration of system components: a) generic configuration, b) multi-resolution real-time 3D thermal imaging system components configuration.*

time 3D thermal imaging system is a novel approach based on our previous work *(12,15)*. The system combines these two previously developed 3D scanning techniques of complementary specifications, to produce a system capable of acquiring 3D thermograms at multiple resolutions and acquisition latencies. A generic depiction of such a system is presented in Figure 1(b).

2.1. Static 3D Thermal Imaging Component

The 3D thermal imaging system presented in *(12)* combines a 3D scanner with a thermal measurement camera, to produce high-resolution 3D thermal models of static subjects. The 3D scanner is comprised of a Digital Light Processing (DLP) projector and a digital RGB camera, Figure 2. Although this system enables the acquisition of high quality 3D thermal models, one of its great limitations is the high latency of the 3D scanning process.

2.2. Dynamic 3D Thermal Imaging Component

The imaging system presented in *(15)* enables the construction of 3D thermal models in real-time at rates of 30

Figure 2. *Configuration of the static 3D thermal imaging component. The component consists of a high-resolution RGB camera, a DLP projector and a thermal measurement camera.*

Figure 3. *Configuration of the dynamic 3D thermal imaging component. The component consists of a RGB camera, a depth camera and a thermal measurement camera.*
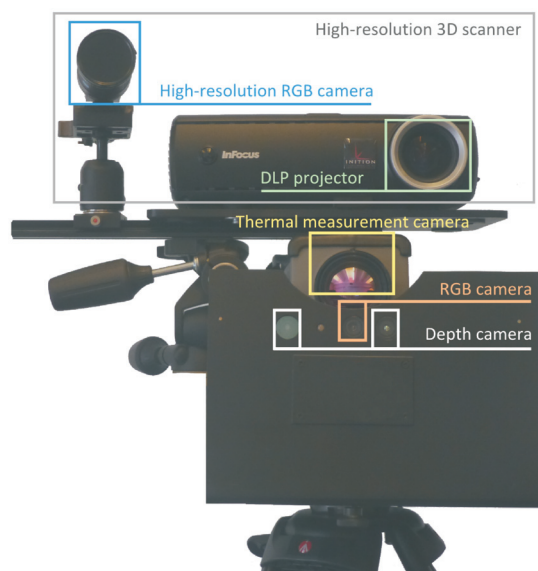

Figure 4. *Implementation of the multi-resolution real-time 3D thermal imaging system.*

frames per second. The system consists of a near-infrared (NIR) projector, NIR camera, RGB camera and a thermal measurement camera, Figure 3. A great advantage of this system is its high acquisition rate, which enables dynamic 3D thermal analysis of a human subject in movement. However, the downside of the system is the relatively low resolution for 3D model acquisition.

2.3. Implementation of the Multi-Resolution Real-Time 3D Thermal Imaging System

Each of the two presented systems can be used for 3D thermal imaging, however, their specifications differ in acquisition rates and quality of output models, which may limit their application under certain conditions. Comparison of these two subsystems is presented in Table 1. In order to exploit their mutual benefits, these subsystems have been combined into a single system. The implementation of the multi-resolution real-time 3D thermal imaging system is shown in Figure 4.

SYSTEM CALIBRATION

Calibrating a single camera can be performed in several different ways *(16, 17, 18)*. Calibration of the system components described in this work is based on the pinhole camera model extended for stereo calibration of the RGB and thermal cameras with the depth camera, similar to the calibration process described in *(19)*. Calibration of a single camera consists in determination of intrinsic and extrinsic parameter matrices, which transform a point from the homogeneous 3D space coordinates to a homogeneous 2D point on the imaging plane. The matrix of intrinsic parameters contains the principal point (u_0, v_0), the focal length f_X and the scaled focal length $f_Y = k\,f_X$, where k is the aspect ratio of a pixel *(20)*, depicted on Figure 5. The matrix of extrinsic parameters contains the external position and orientation of the camera in the 3D world, in the form of rotation and translation components. To determine the values of these parameters, a maximum likelihood solution can be found, as shown in *(16, 19)*.

In order to calculate the calibration parameters of the cameras, reference points have to be determined. Point selection tends to be a difficult challenge in the cases of thermal *(21, 22)* and depth cameras *(17)*, as the flat printed-out checkerboard cannot be distinguished by these modalities. Therefore, in our previous work, a novel calibration pattern that is visible to each of the three implemented modalities has been presented *(15)*. The pattern is given as a flat board made out of a thin thermal insulation material, containing rectangularly shaped holes cut through the board in a checkerboard pattern, Figure 6. The reference points are selected from a series of images of the same scene, taken simultaneously by each camera present in the system.
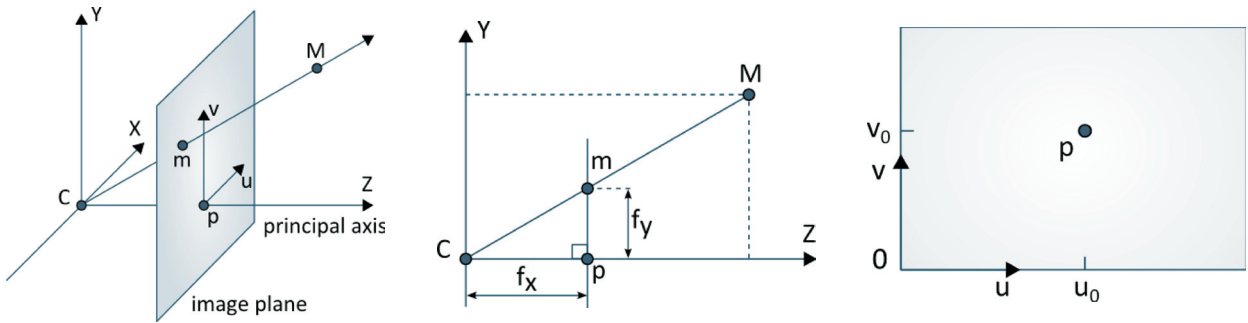
Figure 5. *Depiction of the pinhole camera model: a) relation between the camera position and the imaging plane in 3D space, b) view of the ZY-plane of the same coordinate system, c) imaging plane with the principal point.*
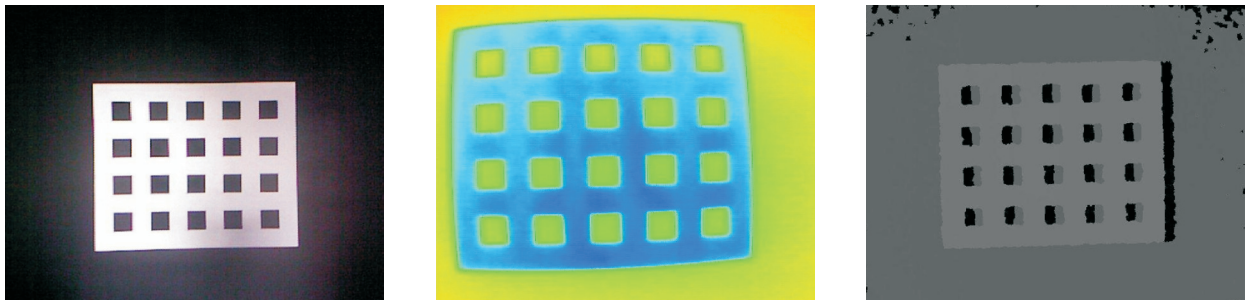

Figure 6. *Calibration pattern as seen by: a) RGB camera, b) thermal camera, c) depth camera.*
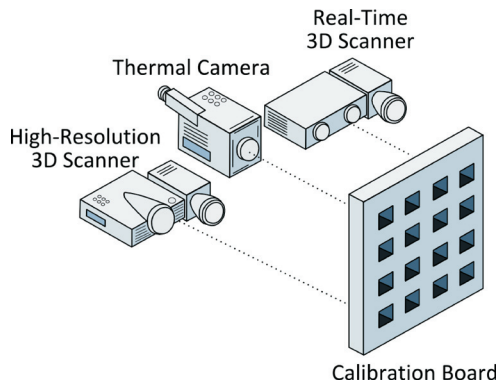

Figure 7. *Stereo calibration of system components.*

The multi-resolution real-time system presents a complex composition of three imaging modalities: depth camera, 3D scanner and thermal measurement camera. Each component is calibrated in a manner analogous to the previously described calibration procedure, Figure 7.

3. TOWARDS STANDARDISATION OF HUMAN BODY 3D THERMAL MODELS

In order to enable reproducibility and comparison of different human body 3D thermal models, a standardisation procedure is required. To provide sufficient quality and suitability for standardisation of full human body 3D thermal models, a novel concept of standardisation pro-

cedure has been presented in the scope of this work. A general workflow of the multi-resolution real-time 3D thermal imaging system improved with standardisation and refitting principles is shown on the Figure 8.

3.1. Standardisation Procedure Concept

Standardisation procedure concept is based on finding correspondences between a scanned *3D Thermal Model* of a human subject and a *Reference 3D Model*. The workflow of the standardisation procedure concept is depicted in Figure 9.
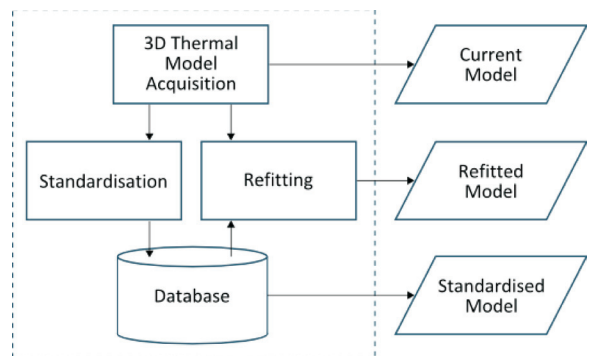

Figure 8. *The general workflow of the standardisation system for human body 3D thermal models.*
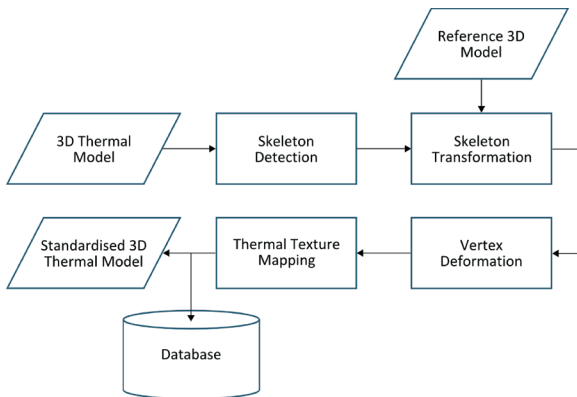
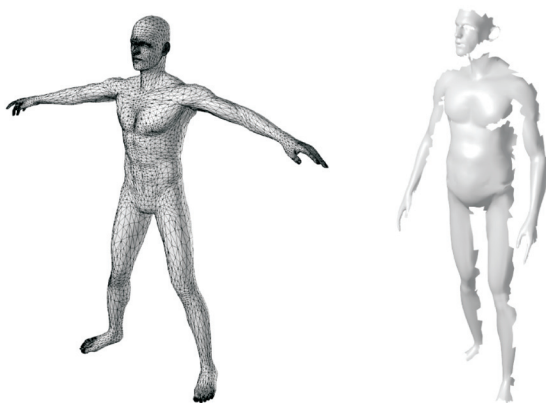**Figure 9.** *Workflow of the standardisation procedure.*

Figure 10. *Human body 3D models of: a) the designed triangular template 3D model of the human body, used for standardisation procedure, b) the high-resolution 3D scan sample.*

Reference 3D Model is predefined as a closed triangulated 3D mesh based on real human body 3D scans with additional manual processing. To provide higher quality of standardisation, the template model is required to contain a large amount of surface polygons, Figure 10(a). The scanned 3D human model is also given as a triangulated 3D mesh providing only the reconstruction from a single point of view, Figure 10(b).

A scanned 3D thermal model is presented to the *Skeleton Detection* process. Skeleton detection of the observed human subject is used for the coarse step of template model transformation. Robust and efficient skeletal detection algorithm that can predict the 3D positions of body joints from a single depth image without any additional temporal information is presented *(14)*. Detected body joints are used for calculating affine transformations of skeleton bones, where each bone is defined by two body joints.

The coarse transformation of the template model is performed in the *Skeleton Transformation* process of the workflow, where the shape of template's skeleton is modified to closely match the skeleton shape of the scanned 3D model. These modifications include affine transformations of skeleton bones, such as scaling of the skeleton bones for models size compensation, and also rotation and translation of each skeleton bone performed through skeleton kinematics. The template model is first scaled by a factor γ, as shown by equation (1):

$$\gamma = \frac{\left| l_{s,SCANNED} \right|}{\left| l_{s,TEMPLATE} \right|} = \frac{\left| p_{shoulder,SCANNED} - p_{hip,SCANNED} \right|}{\left| p_{shoulder,TEMPLATE} - p_{hip,TEMPLATE} \right|} \tag{1}$$
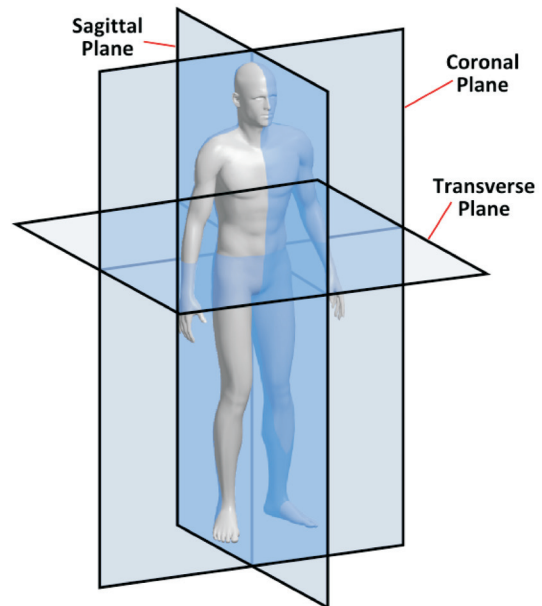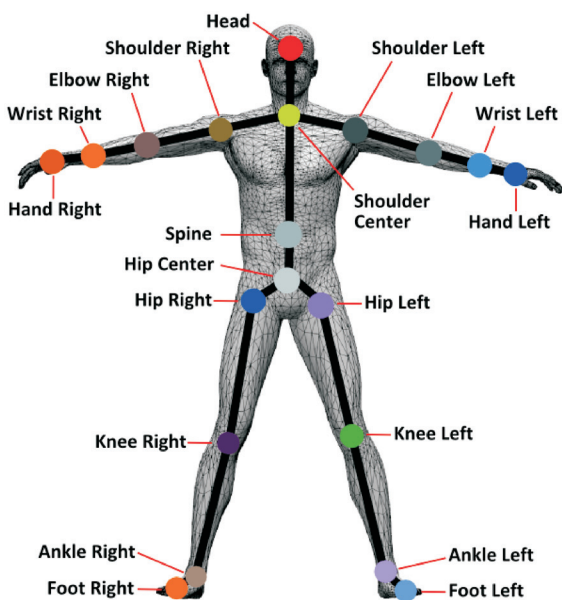

Figure 11. *Illustration of human body space and skeleton joints: a) skeleton model representation of the human body, where points represent joints, while the lines connecting them are the bones of the skeleton, b) sagittal, coronal and transverse plane of the human body.*

where γ represents the ratio of spinal bone lengths of the scanned and the template model, l_s is the length of a spinal bone, and p is the coordinate of a joint in 3D space. The spinal bone of a skeleton is determined by the shoulder-centre and the hip-centre joints of the skeleton, as shown on Figure 11(a). After scaling, the template model is translated and oriented, so that its spinal bone joints lie at the same coordinates as the ones of the scanned 3D model. Additionally, the template model needs to be rotated around the spinal bone vector to match its coronal plane to that of the scanned 3D model, Figure 11(b). The coronal plane of the model is determined by fitting a plane in 3D space through the four joints of a model: left and right hip, hip centre and shoulder centre, Figure 11(a). Left and right shoulder joints have been omitted from the regression procedure because of the wide range of positions that they can be oriented in. After fitting the coronal plane of template to the scanned 3D model, joint adjustment for pose estimation is performed. Bones of the template model are then scaled to the size of the corresponding bones of the scanned model. Last step of the skeleton transformation process includes the use of skeleton kinematics to adjust the positions of the template model's joints to match those of the scanned model.

The result of skeleton transformation is a modified 3D template model that estimates the pose of the scanned human body 3D model. However, the surface of the template model still significantly differs from the targeted scanned model. In the next step, the *Vertex Deformation* process, an optimisation procedure is applied to the template mesh, where the goal of the optimisation is the minimisation of differences between the scanned and the template model's meshes *(23, 24)*. A simplified 2D case of the presented 3D optimisation procedure is depicted on Figure 12(a). Matching the surface of a template model onto a target model is detailed described topic *(23, 24, 25)*. The most suitable method for the mesh optimisation procedure is described in *(26)* where the main approach depends on manual marker selection on both the template
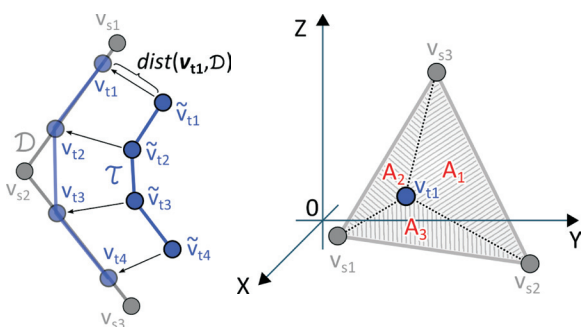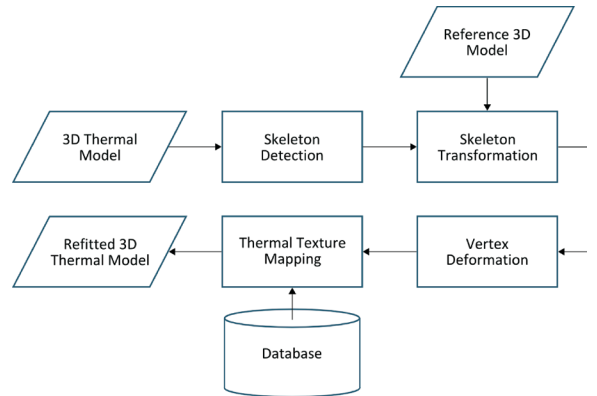

Figure 13. *Workflow of the refitting procedure.*

and the target model. Markers are a set of corresponding points on both models. Markers are intended to prevent the optimisation process getting stuck in a local minimum. In our case, using skeletal transformation to align the meshes prior to the optimisation procedure minimises the chances of ending up in a local minimum. For every vertex v_{ti} of the template model, an affine 4×4 transformation matrix T_i is defined. These transformation matrices determine twelve degrees of freedom for the optimisation search space (nine rotation and three translation parameters). Before running the optimisation procedure, the background polygons are removed from the template model to avoid unwanted deformations that are caused by matching a closed template model to an incomplete scanned model. As in *(26)*, a quasi-Newtonian solver L-BFGS-B can be used to obtain the affine transformation matrices that move all of the points of the template mesh towards the target mesh. The criterion for optimisation function E is used which is defined as the weighted sum of error functions:

$$E_d = \sum_{i=1}^{n} w_i dist^2(T_i v_i, D) \tag{2}$$

$$E_s = \sum_{\{i,j\}|\{v_i, vj\} \in edges(\tau)} \left\| T_i - T_j \right\|_F^2 \tag{3}$$

$$E = \alpha E_d + \beta E_s \tag{4}$$

Here, E_d is the data error function, E_s the smoothness error, and E the objective function. The data error function, E_d, represents the sum of squared distances between each vertex of the template model and the scanned model surface, where n is the number of vertices in the template model, w_i is the weight parameter for controlling the influence of data in different regions, and $dist(\cdot)$ is a function that computes the distance to the closest compatible point on the target model's surface D. The smoothness error function ensures that the adjacent parts of the template surface are not mapped to disparate parts of the scanned model surface. The E_s term also encourages that

Figure 12. *Illustration of the Vertex Deformation process: a) matching the surface of the template model τ to the surface of the scanned model D, b) areas of the triangle used for calculating the barycentric coordinates of a point v_{t1} inside a triangle $\Delta v_{s1} v_{s2} v_{s3}$.*

<div style="text-align:center">

TABLE 1

Comparison of system component characteristics.

</div>

	High-resolution 3D thermography system	Real-time 3D thermography system
Acquisition speed (s)	~ 1	~ 0.05
Distance form object (m)	0.7 – 4.5	1.3 – 4.5
Resolution (mm)	~ 0.5 at minimum distance ~ 3 at maximum distance	~ 0.5 at minimum distance ~ 25 at maximum distance
Accuracy (mm)	~ 0.1	~ 30
Potential applications	Analysis of a very slowly changing or static processes with high-resolution Medical applications - detection of inflamed parts, asymmetric distribution of temperature Industrial applications - monitoring process in larger intervals	Possibility of analysis of dynamic processes with a lower resolution Medical Applications - analysis of movement, rehabilitation, sports medicine Industrial applications - monitoring rapidly changing processes Static analysis is inherently supported

the similarly-shaped features are mapped to each other. The complete objective function E is given as the weighted sum of E_d and E_s, where α and β weights are varied, so that features of the template mesh move freely and match up in the early stages of the optimisation, after which the data term is allowed to dominate.

In *Thermal Texture Mapping* process, thermal image from scanned 3d thermal model is textured onto the template model. For this mapping a texture coordinates of the thermal image need to be determined for the template 3D model. In the previous step, the template model has been transformed in a way that its vertices lay on the scanned model's surface polygons. For one specific vertex of the transformed template model, a single polygon of the scanned model can be identified, such that the vertex lays on that polygon, as illustrated on Figure 12(a). Each vertex of the scanned 3D thermal model has texture coordinates assigned to it during the scanning process. The texture coordinates of the transformed template model's vertex can be obtained through barycentric coordinates. Barycentric coordinates are a form of general homogeneous coordinates that are used in computer graphics and many branches of mathematics. For any point v_t inside an arbitrary triangle $\Delta v_{s1} v_{s2} v_{s3}$, there exist three numbers λ_1, λ_2 and λ_3, such that:

$$v_t = \lambda_1 v_{s1} + \lambda_2 v_{s2} + \lambda_3 v_{s3} \tag{5}$$

In equation (5) v_{s1}, v_{s2} and v_{s3} are the vertices of a scanned model's polygon in Cartesian coordinate space, and λ_1, λ_2 and λ_3 are barycentric coordinates. With one additional condition (6):

$$\lambda_1 + \lambda_2 + \lambda_3 = 1 \tag{6}$$

the barycentric coordinates are defined uniquely for every point inside the triangle. Equation (5) can then be written as:

$$v_t = v_{s1} + (v_{s2} - v_{s1}) \cdot \lambda_2 + (v_{s3} - v_{s1}) \cdot \lambda_3 \tag{7}$$

Parameters λ_1, λ_2 and λ_3 represent, respectively, areas A_1, A_2 and A_3 of the triangle $\Delta v_{s1} v_{s2} v_{s3}$ depicted in Figure 12(b), that are normalised to the area of the entire triangle A_Δ. The area of an arbitrary triangle $\Delta v_{s1} v_{s2} v_{s3}$ is calculated by equation (8):

$$A_\Delta = \frac{1}{2} \left\| (v_{s2} - v_{s1}) \times (v_{s3} - v_{s1}) \right\| \tag{8}$$

The values of λ_1, λ_2 and λ_3 can then be obtained through equations (9)-(11).

$$\lambda_2 = \frac{A_2}{A_\Delta} = \frac{\left\| (v_{s1} - v_{s3}) \times (v_t - v_{s3}) \right\|}{\left\| (v_{s2} - v_{s1}) \times (v_{s3} - v_{s1}) \right\|} \tag{9}$$

$$\lambda_3 = \frac{A_3}{A_\Delta} = \frac{\left\| (v_{s2} - v_{s1}) \times (v_t - v_{s1}) \right\|}{\left\| (v_{s2} - v_{s1}) \times (v_{s3} - v_{s1}) \right\|} \tag{10}$$

$$\lambda_1 = 1 - \lambda_2 - \lambda_3 \tag{11}$$

Given the barycentric coordinates of a point and the three vertices that define a triangle, Cartesian coordinates of that point can be obtained by equations (5) or (7). Once calculated in vertex domain, the barycentric coordinates can be used to obtain correct texture coordinates of a template model's vertex in a 2D image. Using the described method, thermal image can be correctly mapped on each vertex of the template model.

3.2. Refitting standardised 3D Thermal Models

Reverse process of standardization is called *Refitting* process, Figure 13. Refitting involves reprojecting the texture coordinates of a standardized 3D thermal model to the corresponding regions of scanned 3D human body

model. The workflow is the same as one for the standardization procedure. A transformation of the template model is performed, where each vertex of the template model is projected and approximately mapped onto the surface of the scanned model. Since the transformation between the template and the scanned model is known, the inverse process of refitting can be performed.

The result of the refitting process is given in the form of a scanned 3D model with an arbitrary thermal image mapped as a texture on its surface. The arbitrary thermal image can be taken from any previous standardized measurement. The power of utilization of this procedure is that thermal measurements of one or more subjects can be analyzed and compared regardless of the shape of the subject's body. Therefore, the procedure provides the possibility of finding correspondences in multiple 3D thermograms, which can provide for novel and important diagnostic methods.

3.3. Database of Standardised 3D Thermal Models

The results of the standardisation procedure, together with intermediate results, are stored in the database for later use. The idea of the database is to collect the standardised measurement data from one or more human subjects to provide several key benefits, including:

- Measurement reproducibility,

- Monitoring the development of a medical condition of a single patient through time,

- Automatic and semiautomatic (computer supported) diagnostics and medical condition classification,

- Comparison of a large dataset of measurements for detection of abnormal deviations in human body temperatures.

To provide the information for the following analyses of obtained measurements, a single database entry contains several useful information, including:

- Original scanned human 3D thermal model acquired with either of the 3D thermal imaging components (depends on the application),

- Calculated skeleton transformation parameters,

- Calculated vertex deformation parameters for model matching,

- Standardised human body 3D thermal model in the form of 2D thermal images and corresponding set of texture coordinates of a template 3D human body model,

- Metadata – subject's information and medical conditions.

A potential application of the system standardisation concept is presented in continuation, the detection and annotation of regions of interest (ROI). Specifying regions of interest on a human subject's 3D thermal model depends on the context of the concrete application.

ROI Detection and Annotation process intends to delimit the borders of a ROI. There are three approaches in which regions of interest can be determined. The first one is based on the analysis of 2D thermal images, which is very practical in cases when temperature of the body exhibits rapid localised changes. These inflamed areas are easily detected using common image processing techniques, such as image segmentation and edge detection. Thermal image analysis can be performed completely automatically, or by manual selection of a specific area for inflammation localisation. The coordinates of an inflammation's border can be determined in 3D space using defined texture coordinates of standardised human body 3D thermal model. The second approach for ROI detection is based on the analysis of human body 3D thermal model, both scanned and standardised. Manually selected ROI borders of the scanned human body 3D thermal model can be converted to the standardised 3D thermal model space by using known texture mapping parameters calculated in standardisation procedure. The third approach is given as the combination of the former two: 2D thermal image features and spatial characteristics of 3D model of the subject's body. Once identified on the template model, ROI location can be compared with any other standardised 3D thermal model that has been acquired, thus providing the option of monitoring the temperature of a specific region over time, or comparison of that region with the scans from several different human subjects.

4. CONCLUSION

We advanced a 3D thermography imaging standardization technique to allow quantitative data analysis. Medical Digital Infrared Thermal Imaging is very sensitive and reliable mean of graphically mapping and display skin surface temperature. It allows doctors to visualise in colour and quantify temperature changes in skin surface. The spectrum of colours indicates both hot and cold responses which may co-exist if the pain associate with an inflammatory focus excites an increase in sympathetic activity. However, due to thermograph provides only qualitative diagnosis information, it has not gained acceptance in the medical and veterinary communities as a necessary or effective tool in inflammation and tumour detection. Here, our technique is based on the combination of visual 3D imaging technique and thermal imaging technique, which maps the 2D thermography images on to 3D anatomical model. Then we rectify the 3D thermogram into a view independent thermogram and conform it a standard shape template. The combination of these imaging facilities allows the generation of combined 3D

and thermal data from which thermal signatures can be quantified.

This paper presents novel multi-resolution real-time 3D thermal imaging system as potential solution for the human body thermal standardisation. The system consists of a high-resolution offline 3D scanner and a real-time low-resolution 3D scanner, both of them paired together with a thermal imaging camera. The real-time scanning component of the system provides the possibility of tracking the movement of a human subject for automatic ROI detection and dynamic motion compensation, while the high-resolution component provides acquisition of detailed 3D thermal models which are more suitable for analysis.

The emphasis of this paper is the presentation of the novel concept of the standardisation of human body 3D thermal models, captured by multi-resolution real-time 3D thermal imaging system. The standardisation system is composed from *Standardisation* and *Refitting* procedures. The standardisation procedure consists of four different processes: *Skeleton Detection*, *Skeleton Transformation*, *Vertex Deformation* and *Thermal Texture Mapping* process. Detected skeleton used in *Skeleton Transformation* simplifies optimisation process in *Vertex Deformation* preventing the algorithm to end in local min.

Presented concept of 3D thermal model standardisation enables novel and practical methods for model comparison and analysis. Examples of such analyses include detection of differences between multiple 3D thermal models (obtained from one or more individuals) for training classifiers, automatic detection of inflammations, monitoring and diagnosis of various medical conditions that manifest through temperature change, etc.

However, the presented system concept is limited by several constraints. To enable the standardisation procedure, the whole body of the subject has to fit in the recorded scene. As a consequence, the subject needs to be positioned far enough from the imaging system, which reduces the number of details that can be reconstructed. Thus, the greatest limiting factors for high-quality analysis are the resolutions of the 3D scanning components, and the resolution of the thermal camera. Additionally, the depth estimation error grows with the distance from the 3D scanner and needs to be taken into account when constructing the system for specific applications. Standardisation procedure includes optimisation process which requires significant computing power for calculation making system incapable for real-time usage. This makes system limited only to the offline dynamic analysis of the captured human body 3D thermal models. Other limitations include the occlusion of hidden body parts when only one 3D thermal model is acquired, standardisation error due to the model transformation and deformation process, speed of acquisitions, and the compactness of the system's design.

Thus, the proposed system can be valuable for current and future medical applications, for modelling and simulation of biological and physiological processes in human body, as well as for an important potential addition to the concept of the Virtual Physiological Human model. The new 3D thermographic technology represents an enhanced imaging which provides quantifiable multidimensional and multispectral data sets. The measurement of temperature variation along the surface of the body, provided by multimodal imaging, is becoming a valuable auxiliary tool for the early detection of many medical conditions. Multidimensional and multispectral visualization and the related field of visual analytics are opening the doors towards new interactive medical visualization technologies. Interactive visualization integrated with analysis and reasoning techniques permits new modes of exploration, discovery, reasoning and understanding. 3D thermography has predispositions to improve and define the non-invasive and more economical body condition and Health Imaging technology.

REFERENCES

1. SKALA K, LIPIĆ T, SOVIĆ I, GRBEŠA I 2013 Towards 3D thermal models standardisation for human body in motion, Quantitative InfraRed Thermography Journal, Vol 10, No2,: p 207-221

2. JADIN M S, TAIB S 2012 Recent progress in diagnosing the reliability of electrical equipment by using infrared thermography. *Infrared Physics and Technology 55(4):* 236-245

3. KATEBA B, YAMAMOTOD V, YUA C, GRUNDFESTB W, GRUENA J P 2009 Infrared thermal imaging: A review of the literature and case report. *International Brain Mapping & Intraoperative Surgical Planning Society (IBMISPS) 47:* T154-T162

4. DIAKIDES N A, BRONZINO J D 2008 Medical Infrared Imaging. Taylor & Francis Group, LLC; ISBN: 978-0-8493-9027-2

5. ETEHAD TAVAKOL M, LUCAS C, SADRI S, NG EYK 2010 Analysis of Breast Thermography Using Fractal Dimension to Establish Possible Difference between Malignant and Benign Patterns. *Journal of Healthcare Engineering 1(1):* 27-43

6. HILDEBRANDT C, ZEILBERGER K, RING E F J, RASCHNER C 2012 The Application of Medical Infrared Thermography in Sports Medicine. An International Perspective on Topics in Sports Medicine and Sports Injury; ISBN: 978-953-51-0005-8: 257-274

7. SKALA KAVANAGH H, DUBRAVIĆ A, GRAZIO S, LIPIĆ T AND SOVIĆ I 2011 Computer supported thermography monitoring of hand strength evaluation by electronic dynamometer. *Period biol 113(4):* 433-437

8. HERMAN C, CETINGUL M P 2011 Quantitative visualization and detection of skin cancer using dynamic thermal imaging. *Journal of Visualized Experiments 51:* e2679

9. RING E F J, AMMER K, JUNG A, MURAWSKI P, WIECEK B, ZUBER J, ZWOLENIK S, PLASSMANN P, JONES C, JONES B F 2004 Standardization of Infrared Imaging. *Proceedings of 26th Annual International Conference of the IEEE Engineering in Medicine and Biology Society 1:* 1183-1185. San Francisco, California.

10. SANSONI G, TREBESCHI M, DOCCHIO F 2009 State-of-The-Art and Applications of 3D Imaging Sensors in Industry, Cultural Heritage, Medicine, and Criminal Investigation. *Sensors 9(1):* 568-601

11. YANG R, CHEN Y 2011 Design of a 3-D Infrared Imaging System Using Structured Light. *IEEE Transactions on Instrumentation and Measurement 60(2):* 608-617

12. GRUBIŠIĆ I, GJENERO L, LIPIĆ T, SOVIĆ I, SKALA T 2011 Medical 3D thermography system. *Period biol 113(4):* 401-406

13. JU X, NEBEL C, SIEBERT J P 3D 2004 Thermography imaging standardization technique for inflammation diagnosis. *Proceedings of the international society for optics and photonics 5640:* 266-273. Beijing, China.

14. SHOTTON J, FITZGIBBON A, COOK M, SHARP T, FINOCCHIO M, MOORE R, KIPMAN A, BLAKE A 2011 Real-Time Human Pose Recognition in Parts from Single Depth Images. *Proceedings of Computer Society Conference on Computer Vision and Pattern Recognition:* 1297-1304. Colorado Springs.

15. SKALA K, LIPIĆ T, SOVIĆ I, GJENERO L, GRUBIŠIĆ I 2011 4D thermal imaging system for medical applications. *Period biol 113(4):* 407-416

16. ZHANG Z A 2000 Flexible New Technique for Camera Calibration. *IEEE Transactions on Pattern Analysis and Machine Intelligence 22(11):* 1330-1334

17. HERRERA C D, KANNALA J, HEIKKILA J 2011 Accurate and Practical Calibration of a Depth and Color Camera Pair. *Proceedings of Computer Analysis of Images and Patterns 6855:* 437-445. Seville, Spain.

18. STONE E E, SKUBIC M 2011 Evaluation of an Inexpensive Depth Camera for Passive In-Home Fall Risk Assessment. *Proceedings of 5th International Conference on Pervasive Computing Technologies for Healthcare:* 71-77. Dublin, Ireland.

19. ZHANG C, ZHANG Z 2011 Calibration between depth and color sensors for commodity depth cameras. *Proceedings of International Workshop on Hot Topics in 3D, in conjunction with IEEE International Conference on Multimedia & Expo:* 1-6. Barcelona, Spain.

20. SANDBERG D 2011 Model-Based Video Coding Using a Colour and Depth Camera. *Proceedings of the 2011 International Conference on Digital Image Computing.* Noosa, Australia.

21. SUN W, YANG X, XIAO S, HU W 2008 Robust Recognition of Checkerboard Pattern for Deformable Surface Matching in Multiple Views. *Proceedings of High Performance Computing and Simulation Conference.* Cyprus.

22. AKSENOV P, CLARK I, GRANT D, INMAN A, VARTIKOVSKI L, NEBEL J-C 2003 3D thermography for quantification of heat generation resulting from inflammation. *Proceedings of 8th 3D Modelling symposium.* Paris, France.

23. STATEN M L, OWEN S J, SHONTZ S M, SALINGER A G, COFFEY T S 2011 A comparison of mesh morphing methods for 3D shape optimization. *Proceedings of 2011 International Meshing Roundtable:* 293-312. Paris, France.

24. ALEXA M 2002 Recent Advances in Mesh Morphing. *Computer Graphics Forum:* 173-196

25. SCHNEIDER D C, EISERT P 2009 Fitting a Morphable Model to Pose and Shape of a Point Cloud. *Proceedings of Vision, Modeling and Visualization:* 93-100. Braunschweig.

26. ALLEN B, CURLESS B, POPOVIĆ Z 2003 The space of human body shapes: reconstruction and parameterization from range scans. *Proceedings of Special Interest Group on GRAPHics and Interactive Techniques 22(3):* 587-594. San Diego, California.